Nanomed J. 12(1): 70-84, Winter 2025

RESEARCH PAPER

Mycofabrication of selenium and tellurium nanoparticles by using *Penicillium rubens*: *In-vitro* physicochemical, antimicrobial, antioxidant, urease inhibitory, thrombolytic and anticoagulant performance

Hamed Barabadi [1]*, Fatemeh Ashouri [1], Kamyar Jounaki [1], Reza Jahani [2], Salimeh Amidi [3], Omid Hosseini [4], Melika Kamali [1]

[1]Department of Pharmaceutical Biotechnology, School of Pharmacy, Shahid Beheshti University of Medical Sciences, Tehran, Iran
[2]Department of Toxicology and Pharmacology, School of Pharmacy, Shahid Beheshti University of Medical Sciences, Tehran, Iran
[3]Department of Medicinal Chemistry, School of Pharmacy, Shahid Beheshti University of Medical Sciences, Tehran, Iran
[4]Shahid Beheshti University of Medical Sciences, Tehran, Iran

ABSTRACT

Objective(s): This study aimed to investigate the extracellular synthesis of colloidal nanosized selenium (SeNPs) and tellurium (TeNPs) particles using the supernatant of Penicillium rubens, and to evaluate their biological activities.

Materials and Methods: Colloidal SeNPs and TeNPs were characterized using energy-dispersive X-ray spectroscopy (EDX), field emission scanning electron microscopy (FE-SEM), dynamic light scattering (DLS), and Fourier transform infrared spectroscopy (FT-IR) analysis. Biological tests included antimicrobial tests using the well diffusion assay, broth microdilution assay, and flow cytometry, as well as antioxidant, urease inhibitory, thrombolytic, and anticoagulant assays.

Results: The average hydrodynamic diameters of the synthesized SeNPs and TeNPs were determined to be 43.91 nm and 37.17 nm, respectively. TeNPs exhibited significant antibacterial activity against *Escherichia coli* with an inhibition zone (IZ) of 27 mm and a minimum inhibition concentration (MIC) of 2.5 $mg.mL^{-1}$. Flow cytometry analysis showed a dose-dependent bacterial cell death with TeNPs. However, SeNPs did not display any antibacterial activity against Escherichia coli. Neither TeNPs nor SeNPs showed antimicrobial properties against *Staphylococcus aureus* and *Candida albicans*. Both TeNPs and SeNPs exhibited antioxidant properties, inhibiting 43.90±1.98% and 57.93±2.20% of DPPH free radicals at 1 $mg.mL^{-1}$, respectively. Additionally, the mycofabricated NPs displayed a dose-dependent urease inhibitory activity with maximum inhibition of 63.81±1.69% and 46.95±3.39% at 1 $mg.mL^{-1}$, respectively. However, neither TeNPs nor SeNPs showed thrombolytic or anticoagulant activity at 1 $mg.mL^{-1}$.

Conclusion: Our findings demonstrate that mycofabricated nanosized selenium and tellurium particles possess significant antioxidant and urease inhibitory properties, with TeNPs showing promising antibacterial activity against *E. coli. T*hese results suggest potential applications for these nanoparticles in biomedical and agricultural fields.

Keywords: *Biosynthesis, Nanoparticles, Penicillium rubens, Pharmaceutical research*

How to cite this article

Barabadi H, Ashouri F, Jounaki K, Jahani R, Amidi S, Hosseini O, Kamali M. Mycofabrication of selenium and tellurium nanoparticles by using Penicillium rubens: In-vitro physicochemical, antimicrobial, antioxidant, urease inhibitory, thrombolytic and anticoagulant performance. Nanomed J. 2025; 12(1): 70-84. DOI: 10.22038/nmj.2024.77665.1896

INTRODUCTION

Nanobiotechnology is a cutting-edge field that merges the principles of nanotechnology and biology to explore the fascinating world of nanosized materials. By manipulating matter at this tiny level, specifically 1–100 nm, scientists can engineer materials and devices with unique properties and uncover new insights into the fundamental performance of biological systems [1]. Nanobiotechnology has numerous applications across various sectors,

* *Corresponding author: Emails: barabadi@sbmu.ac.ir; barabadi.87@gmail.com*

Note. This manuscript was submitted on January 22, 2024; approved on June 22, 2024

including medicine, energy, and environmental conservation. This interdisciplinary approach has the potential to revolutionize industries and improve the quality of life by providing efficient and sustainable solutions to complex issues [2]. There are several approaches for synthesizing nanoparticles (NPs), including chemical, physical, and biological approaches. The chemical approach involves using chemical reactions to produce NPs, while the physical method involves physical processes such as vapor condensation or laser ablation [3]. However, an increasingly popular and superior synthesis approach of NPs is based on biological resources. Biological fabrication of NPs, also known as green synthesis, utilizes living organisms such as bacteria, fungi, plants, algae, or even enzymes. This approach offers several advantages over traditional methods. Firstly, it is environmentally friendly because it does not involve toxic chemicals and harmful byproducts associated with chemical synthesis [4]. Secondly, it is cost-effective as it eliminates the need for expensive equipment and complex procedures [5]. Additionally, biological synthesis facilitates the manufacturing of NPs with precise control over their size, shape, and composition, thereby playing a significant role in their targeted applications. Furthermore, biological synthesis offers a unique opportunity to harness the natural processes and mechanisms of living organisms. This approach can lead to the production of NPs with enhanced properties and functionalities compared to those obtained through conventional methods [6]. For example, biological synthesis can result in NPs with improved stability, biocompatibility, and bioactivity, making them highly suitable for biomedical applications [7].

Fungi, among various biofactories, have gained significant attention owing to their unique characteristics, such as their high tolerance to metal ions, which allows for effective conversion into NPs. They also possess a high surface area, enabling better interaction with metal ions and subsequent NPs preparation. Moreover, fungus-mediated synthesis offers advantages such as scalability, cost-effectiveness, and ease of handling [8]. Fungi can be easily cultured and scaled up for large-scale production of NPs [9]. They also have the ability to produce large amount of biomolecules and synthesize NPs under ambient conditions, eliminating the need for complex procedures, costly tools, and additional capping or stabilizing agents [4]. Furthermore, fungal synthesis allows for the fabrication of NPs with desired characteristics. Fungi can be manipulated to fabricate NPs with specific and enhanced properties by altering growth conditions or introducing specific metal precursors. This control over NP properties is crucial for tailoring their applications in various fields. Therefore, fungi offer a promising avenue for the fabrication of NPs with enhanced properties, making them a valuable tool in nanobiotechnology and various scientific and technological advancements [10].

Penicillium chrysogenum, recently renamed *P. rubens*, is a fungal species frequently encountered in soil, decomposing organic matter, and indoor environments [11]. This fungus is renowned for its remarkable capacity to generate a wide range of secondary metabolites, encompassing antibiotics and mycotoxins. *P. rubens* has been extensively studied for its potential applications in various fields. Its ability to produce antibiotics, particularly penicillin, discovered by Alexander Fleming in 1928, has been widely utilized in the pharmaceutical industry for the treatment of bacterial infections. This discovery revolutionized medicine, and paved the way for the development of numerous other antibiotics [12, 13]. In addition to its antibiotic properties, *P. rubens* also produces other bioactive compounds with potential therapeutic applications. These include antifungal agents, gene expression agents, and anticancer compounds [14-16]. The exploration of these secondary metabolites has opened up new possibilities for drug discovery and development. Furthermore, *P. rubens* has been studied for its role in bioremediation. This fungus can degrade various organic pollutants, including pesticides and hydrocarbons, making it a potential candidate for environmental cleanup [17]. Overall, the diverse capabilities and bioactive compounds of *P. rubens* make it an important organism for further research and exploration. Recently, the investigation of metal NPs synthesized using green resources has been the focus of many scholars. Biofabricated TeNPs and SeNPs are highly sought because of their distinct properties and immense potential for various applications. Both TeNPs and SeNPs have emerged as possessing strong antioxidant activity. This is due to their capability to effectively scavenge free radicals and hinder oxidative stress. Therefore, they can be regarded as promising candidates for the development of therapeutic agents for various oxidative stress-related diseases, including neurodegenerative disorders, cardiovascular diseases, and cancer [18]. These materials can be used to create

innovative antimicrobial agents and coatings for medical devices. They have demonstrated strong antimicrobial properties and have proven effective against a wide range of pathogens, including fungi, bacteria, and viruses, making them suitable for treating infectious diseases [19, 20]. Furthermore, the utilization of eco-friendly NPs to effectively suppress the activity of various enzymes is a fresh approach for developing enzyme-targeted therapeutics for the treatment of metabolic disorders [21]. Notably, hindering urease, a vital enzyme for *Helicobacter pylori* colonization, can be a novel approach for the development of antibiotics against gastrointestinal diseases given the rapid growth of resistance against conventional drugs [22]. Based on our knowledge, this is the first investigation that intorduce biofabricated TeNPs and SeNPs using *P. rubens* (PTCC 5074) and compare their characteristics and biological properties. Moreover, as far as we know, no previous studies have evaluated the thrombolytic, anticoagulant, and urease inhibitory activity of biosynthesized TeNPs and SeNPs.

MATERIALS AND METHODS

Materials and reagents

The used reagents and chemicals were provided from Sigma-Aldrich, USA.

Collection and documentation of fungal and bacterial strains

The fungus *P. rubens* (PTCC 5074) was obtained from the Department of Pharmaceutical Biotechnology at the School of Pharmacy, Shahid Beheshti University of Medical Sciences (SBMU) in Tehran, Iran. In addition, the microbial strains including *E. coli* (ATCC 25922), *S. aureus* (ATCC 25923), and *C. albicans* (ATCC 10231) were received from the Central Research Laboratories at Shahid Beheshti University of Medical Sciences (SBMU), in Tehran, Iran.

Mycofabrication of colloidal nanosized selenium and tellurium particles

P. rubens was grown in Sabouraud Dextrose Broth (SDB) and incubated at 28 °C and 120 rpm on a rotary shaker for one week. After incubation, the profusely grown fungal mycelia were discarded and 100 mL of fungal supernatant was mixed with 100 mL of 1 mmol.L^{-1} aqueous sodium selenite (Na_2SeO_3) and/or potassium tellurite (K_2TeO_3) solutions in separate Erlen Meyer flasks. The final pH value was adjusted to 9 and the flasks were placed under shaker conditions (120 rpm) at 28 °C until the NPs were fabricated. A negative control was also incubated under the same conditions. Next, the mycofabrication of SeNPs and TeNPs was visually confirmed by a color change in the reaction mixtures to orange and dark-gray, respectively. The NPs were then separated from the colloidal system by centrifuging at 20,000 rpm for 20 min using an ultracentrifuge (Beckman, L90k, USA). The sedimented NPs were washed three times with deionized double-distilled water to increase their purity. Subsequently, the NPs were dried at 40 °C and stored in vials for the remainder of the study.

Structural characterization of colloidal nanosized selenium and tellurium particles

The shape and elemental content of biofabricated SeNPs and TeNPs were investigated using field emission scanning electron microscopy (FE-SEM) (Sigma VP, ZEISS, Germany) at 15 kV, coupled with energy-dispersive X-ray spectroscopy (EDX) analysis. The hydrodynamic diameters of biogenic SeNPs and TeNPs were determined using a Zetasizer Nanoparticle Analyzer equipped with a Zetasizer 3600 instrument made in Malvern, UK, operating at a scattering angle of 90° and a temperature of 25 °C. Furthermore, Fourier-transform infrared (FT-IR) spectroscopy was conducted to identify the chemical groups present on the surfaces of the mycofabricated nanosized particles. To achieve this, a semitransparent disk with a thickness of 2 mm was created by compressing a mixture containing NPs and KBr in a ratio of 1:100 for 2 min. Subsequently, the disk was analyzed using FT-IR (Agilent, Cary 630 model, USA) within the wavelength range of 400-4000 cm^{-1}.

Biological properties of colloidal nanosized selenium and tellurium particles

Antimicrobial properties

Well diffusion assay

To assess the antimicrobial efficacy of biosynthesized SeNPs and TeNPs, a study was conducted using *E. coli* (ATCC 25922) as a reference strain. The IZ assessment was performed using an agar-well diffusion assay. For this experiment, the *E. coli* inoculum was prepared to achieve a cellular density of 10^8 CFU.mL^{-1}. The *E. coli* inoculum was then distributed evenly on the surface of a Mueller Hinton Agar (MHA) plate for inoculation. Next, 100 µL of SeNPs and TeNPs from a stock of 1 mg.mL^{-1} were individually placed into carefully punched wells with a diameter of 8 mm. The agar plates were then incubated at 37 °C for 24 hr. Afterward, the IZ assessment was conducted. The same steps

were followed for *S. aureus* (ATCC 25923) and *C. albicans* (ATCC 10231).

Broth microdilution assay

The MIC value of biogenic SeNPs and TeNPs is defined as the lowest concentration at which the visible growth of a microbial organism is completely inhibited. To determine the MIC, a 96-well microtiter plate was utilized to dispense 100 µL of Mueller Hinton Broth (MHB) medium into twelve wells. Subsequently, 100 µL of the biogenic SeNPs was added to the first well. Then, 100 µL of the components in the first well was transferred to the second one. This sequential procedure was repeated for the remaining wells, from the third to the eleventh. The twelfth well served as the negative control, indicating the absence of nanomaterials. The same steps were followed for TeNPs. After that, a 100 µL suspension of *E. coli* with a concentration of 10^6 CFU.mL^{-1} was added to all wells. Similarly, the MIC of the antibiotic gentamicin was evaluated as the reference standard. Finally, the plates were incubated at 37°C for 24 hr following the mixing of the components. This method was also repeated for *S. aureus* and *C. albicans*.

Quantitative evaluation of cell viability using flow cytometry

In the initial phase, Luria-Bertani (LB) broth was used to culture a reference strain of *E. coli* at a concentration of 10^8 CFU.mL^{-1}. Then, the bacterial strain was exposed to biogenic TeNPs at concentrations of MIC, 10*MIC, and 20*MIC. The antibiotic gentamycin, commonly used as a positive control, was also included in this study. After incubation at 37 °C and 125 rpm for 6 hr, the samples were centrifuged at 8000 rpm for 1 min. The supernatant was then removed and the bacterial plate was washed twice with phosphate-buffered saline (PBS) buffer. The plate was dissolved in a PBS buffer solution and incubated for 2 min with a propidium iodide (PI) dye concentration of 2 µg.mL^{-1}. The plate was analyzed using a flow cytometer (BD FACSCalibur, USA), and the obtained data were evaluated using the FlowJo program (Tree Star, Inc., Ashland, OR, USA).

Antioxidant properties

The radical scavenging ability of SeNPs and TeNPs against the 2,2-diphenyl-1-picrylhydrazyl (DPPH) radical was assessed using the following steps: First, each sample of NPs was prepared at a concentration of 1 mg.mL^{-1} using 90% ethanol. Next, a 1 mL solution of DPPH (0.3 mM) was added to a 2.5 mL sample of NPs (1 mg.mL^{-1}). The absorbance value was measured at 518 nm after a 30-min incubation at room temperature. To make a comparison, the DPPH radical-scavenging capacity of the fungal supernatant was also evaluated. Additionally, the DPPH radical-scavenging ability of ascorbic acid (10 mg.mL^{-1}) was examined as a positive control. The antioxidant potential of TeNPs was similarly evaluated. Finally, the percentage of DPPH scavenging activity of the samples was determined by calculating it using the formula below:

Percentage of DPPH scavenging activity = [(Acontrol – (Asample– Ablank)/(Acontrol)] × 100

In this formula, Acontrol represents the absorbance value of the control, Asample is the absorbance value of the sample, and Ablank refers the absorbance value of the blank sample.

Urease enzyme inhibitory properties

To assess the ability of green fabricated SeNPs and TeNPs for hindering the activity of the urease enzyme, a mixture was prepared. The mixture consisted of 25 µL of urease obtained from *Canavalia ensiformis*, 55 µL of a solution containing 30 mM urea and phosphate buffer (100 mM, pH 7.4), and 5 µL of biological SeNPs and TeNPs. This mixture was then poured into a well of a 96-well microtiter plate. After incubation of the plate for 15 min at 30 °C, 45 µL of solution A (phenol reagent containing 1% phenol and 0.005% W/V sodium nitroprusside) and 70 µL of solution B (alkali reagent containing 0.5% W/V NaOH and 0.1% W/V NaOCl) were added to each well. The wells were further incubated for 50 min at 30 °C, and then, the absorbance peak of the sample was measured at 630 nm. Simultaneously, the urease activity of the NPs was assessed using the indophenol method. In this method, the reaction of phenol, hypochlorite, and NH3 generated a blue indophenol solution as a result of urease function. The results were compared to the colorless control solution with no urease, which contained thiourea as the standard enzyme inhibitor. Finally, the percentage of enzyme inhibition was calculated using the following formula:

(1- (ODsample)/(ODconrtol))×100

Thrombolytic properties

The thrombolytic assay was conducted as

described elsewhere [23]. Briefly, 500 µL of blood from a healthy adult male volunteer was transferred to empty Eppendorf tubes and incubated at 37°C for 30 min to allow clotting. The weight of the blood clot was then measured. Consequently, 100 µL of TeNPs and SeNPs from a stock of 1 $mg.mL^{-1}$ was transferred into the Eppendorf tubes containing the blood clots, followed by another incubation at 37 °C for 90 min. Distilled water was used as a negative control. Finally, the lysed clots were discarded and the percentage reduction in the weight of the remaining clots was measured.

Anticoagulant properties

The anticoagulant assay was conducted according to elsewhere previously described method [24]. Platelet-poor plasma (PPP) was prepared by centrifuging a tube containing sodium citrate and a blood sample from a healthy and adult male volunteer at 1500 g for 15 min. Next, a coagulation analyzer (Coa DATA 501, LABitec, Germany) was employed to assess the activated partial thromboplastin time (aPTT) and the prothrombin time (PT). For the aPTT, prewarmed PPP (45 µL), mycofabricated NPs (5 µL), and aPTT reagent (50 µL) were mixed and incubated at 37 °C for 180 sec. Then, prewarmed calcium chloride (50 µL from a stock solution of 0.025 M) was added to the mixture. The time needed for blood clot formation was recorded using a coagulation analyzer. Additionally, for the PT, prewarmed PPP (45 µL) and mycofabricated NPs (5 µL) were mixed and incubated at 37 °C for 300 s. Then, prewarmed thromboplastin-D (100 µL) was added to the mixture. The time needed for blood clot formation was recorded using a coagulation analyzer.

Statistical analysis

The data was analyzed using GraphPad Prism software (San Diego, CA; version 7.0). One-way Analysis of Variance (ANOVA) and Tukey post-test were employed to determine if there were statistically significant differences in the mean values of multiple groups. The data was presented as the mean ± standard deviation (SD). A confidence level of 95% was used to determine if there was a statistically significant difference between the groups ($P<0.05$).

RESULTS AND DISCUSSIONS

Mycofabrication of colloidal nanosized selenium and tellurium particles

Fig. 1 shows a schematic illustration of green process of mycofabrication of SeNPs and TeNPs.

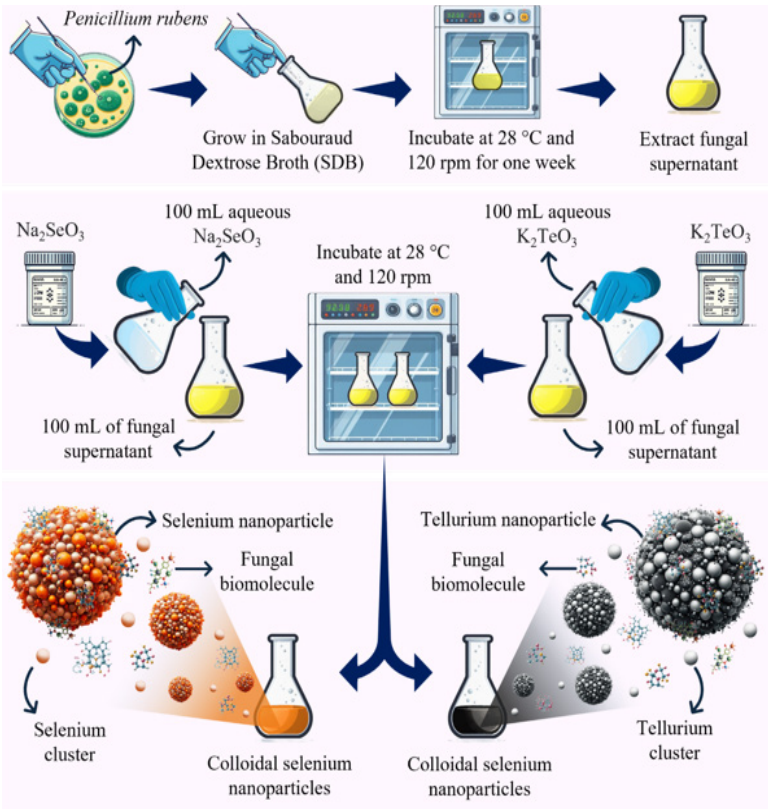

Fig. 1. A schematic illustration of green synthesis of nanosized selenium and tellurium particles resulting in stable colloidal system

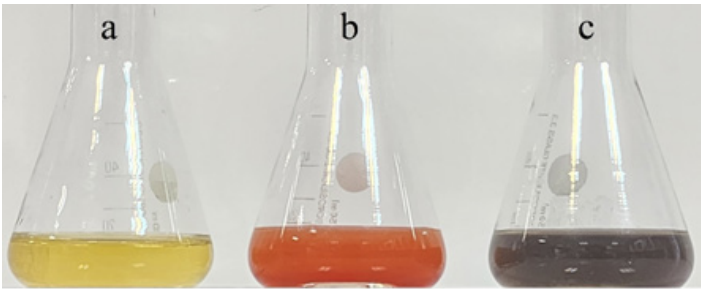

Fig. 2. Color alternation in the reaction mixture after incubation and confirmation of SeNPs and TeNPs biosynthesis. a) *P. rubens* supernatant (negative control); b) biofabricated colloidal SeNPs; c) biofabricated colloidal TeNPs

The fabrication of SeNPs and TeNPs was confirmed by observing the color change in the mixture. The SeNPs changed from pale yellow to reddish orange, while the TeNPs turned dark gray (Fig. 2). This color change is attributed to the surface plasmon resonance (SPR) phenomenon, where the free electrons of the NPs collectively vibrate in response to light in the visible region, resulting in new colors. These color changes provide evidence for the bioreduction of metallic ions into SeNPs and TeNPs. Previous studies have also used different biological resources to produce SeNPs or TeNPs, which aligns with our findings [20, 25-27]. It is important that the specific the mechanism behind the biological synthesis of these NPs is not fully understood. However, one study hypothesized that certain proteins found in the biofactory's supernatant act as reducing agents in the synthesis of SeNPs by *Mariannaea* sp. HJ [28].

Structural characterization of colloidal nanosized selenium and tellurium particles

Biogenic SeNPs and TeNPs were characterized as spherical according to the results from FE-SEM

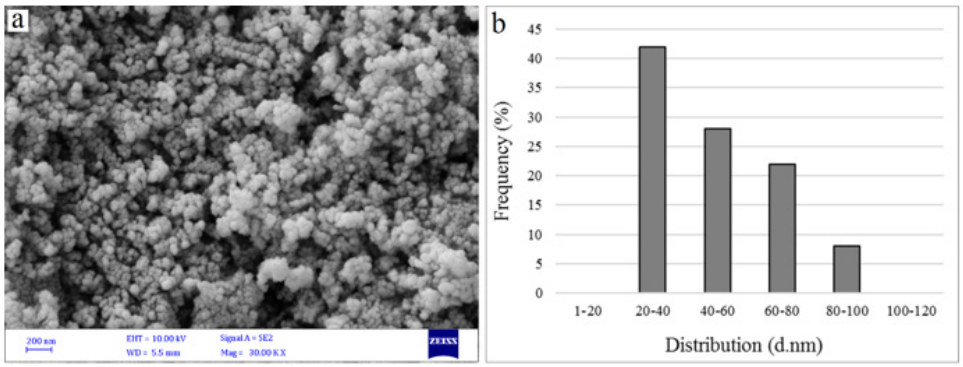

Fig. 3. Structural analysis of the biogenic SeNPs using FE-SEM image (a), and particle size distribution (b) of SeNPs

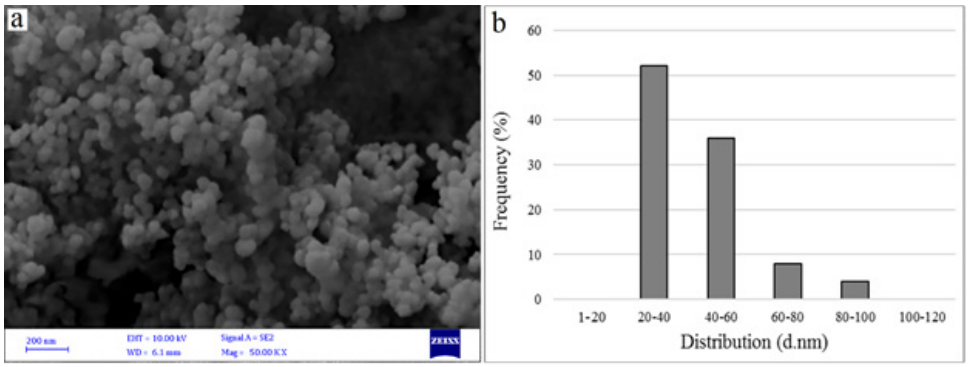

Fig. 4. Structural analysis of the biogenic TeNPs using FE-SEM image (a), and particle size distribution (b) of TeNPs

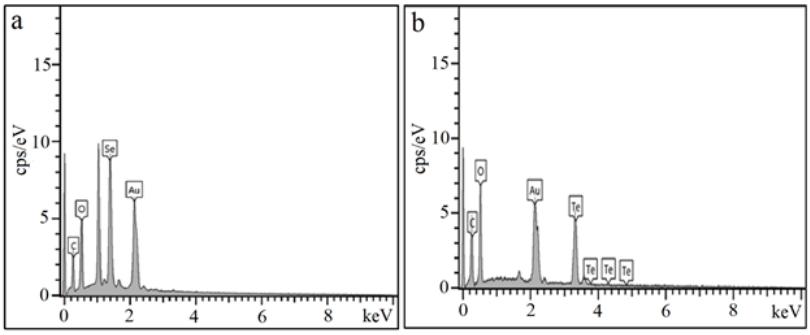

Fig. 5. EDX spectrum of SeNPs (a) and TeNPs (b) representing the elemental composition of NPs

analyses (Fig. 3a and 4a). Besides, Fig. 3b and 4b show the particle size distribution of SeNPs and TeNPs, respectively. The *P. rubens*-mediated NPs exhibited monodispersity and smooth edges. To assess the size distribution of mycofabricated NPs utilizing FE-SEM, we conducted measurements of the diameter of fifty randomly selected particles using ImageJ software. According to FE-SEM images, most of the particles were within the particles sizes of 20 to 40 nm. Additionally, the elemental composition of the biofabricated NPs was determined through EDX results. Intensive signals around 1.4 KeV (Fig. 5a) and 3.3 KeV (Fig. 5b) were identified for selenium and tellurium, respectively. The presence of a gold signal is due to the sample preparation method for EDX, which involves coating the sample with a thin layer of conductive material (e.g., gold) to prevent surface charging. Other peaks may correspond to biological molecules present in the fungal supernatant, serving as stabilizing and capping factors.

As shown in Fig. 6, the average hydrodynamic diameters of green synthesized SeNPs and TeNPs were measured and reported as 43.91 nm (Fig. 6a) and 37.17 nm (Fig. 6b), respectively, using dynamic light scattering (DLS) as a well-established technique for determining the size distribution of colloidal systems. DLS analyzes the Brownian movement of particles and the fluctuations in the intensity of light scattered throughout a colloidal system [29]. Moreover, the DLS spectrum ascertained the polydispersity index (PdI) as a measure of the heterogeneity of a sample based on size. PdI values above 0.7 indicate samples with a broad size distribution (e.g., polydisperse) [30, 31]. In this study, the PdI values of 0.178 and 0.222 were recorded for SeNPs and TeNPs, respectively, indicating a narrow range of size distribution as

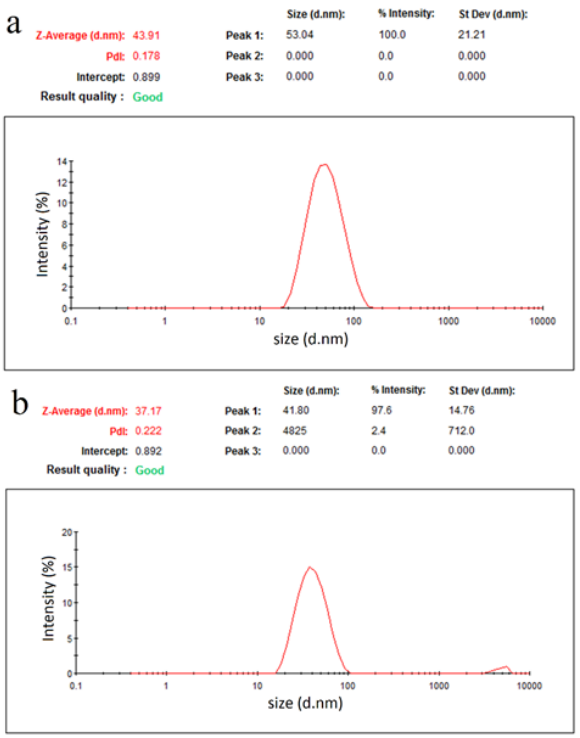

Fig. 6. DLS diagrams of SeNPs (a) and TeNPs (b) representing the average hydrodynamic diameters of 43.91 and 37.17 nm, respectively

they were below 0.7. Moreover, the surface of the NPs generated via mycosynthesis exhibited net negative charges, known as zeta potential, with a value of -25.5 mV for SeNPs (Fig. 7a) and -28.8 mV for TeNPs (Fig. 7b). Zeta potential determines the degree of repulsion between charged particles in a colloidal system. A higher zeta potential value indicates a higher particle charge resulting in significant electric repulsion between the charged particles, which prevents particle coagulation [32].

Furthermore, the presence of biomolecules on

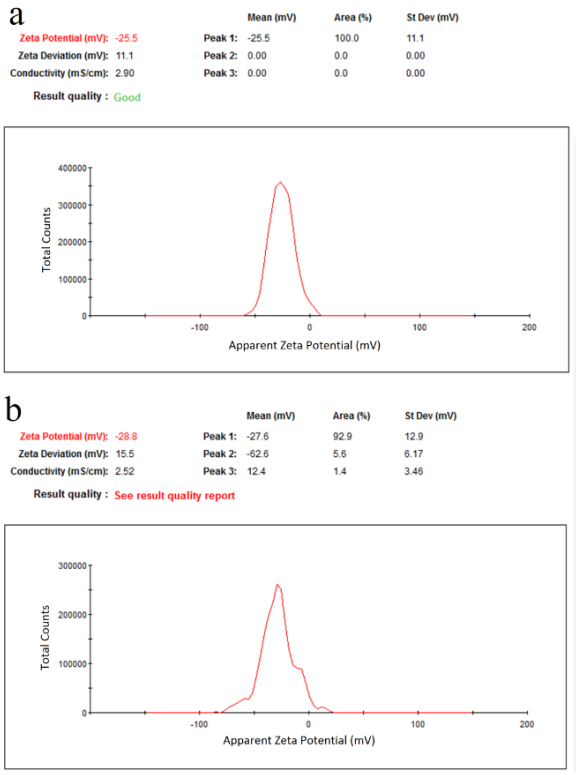

Fig. 7. Zeta potential diagrams of SeNPs (a) and TeNPs (b) representing the values of -25.5 mV and -28.8 nm, respectively

the surface of mycosynthesized SeNPs and TeNPs was determined by studying the FT-IR spectra of the NPs at 450–400 cm^{-1}. Fig. 8a ascertains the FT-IR spectrum of the biogenic SeNPs, with sharp peaks at 3265.15, 2929.69, 1602.76, 1371.66, 1118.20, 1013.84, 931.83, 887.11, 812.56, and 708.19 cm^{-1} corresponding to O-H, C-H, C=C, C-H, C-O, C-O, C=C, C-H, C-H, and C-H stretching bonds, respectively. Fig. 8b ascertains the FT-IR spectrum of the biogenic TeNPs, with sharp signals at 3280.06, 2929.69, 1580.39, 1401.48, 1125.66, 1013.84, 924.38, and 670.92 cm^{-1} indicating the presence of O-H, C-H, C=C, C-H, C-O, C-O, C=C, and C-H functional groups. Likewise, the FI-IR spectrum of the fungal supernatant (Fig. 8c) illustrates the presence of 3309.88, 2974.42, 2929.69, 1602.76, 1453.66, 1408.93, 1371.66, 1118.20, 1051.11, 1013.84, 931.83, 887.11, 812.56, and 656.01 cm^{-1} related to O-H, C-H, C-H, C=C, C-H, C-H, C-H, C-O, C-O, C-O, C=C, C-H, C-H, and C-H stretches, respectively. Consequently, a comparison of the spectra of the NPs with those of the supernatant indicates the presence of similar groups contributed by fungal secreted biomolecules and chemicals capping the NPs.

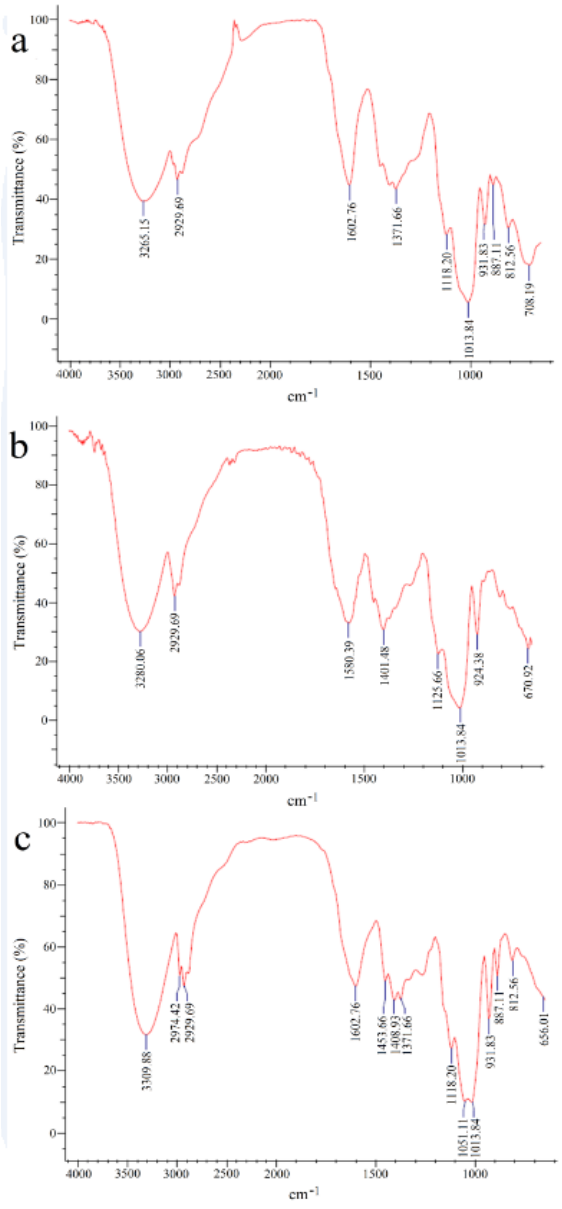

Fig. 8. The FT-IR spectra of a) SeNPs, b) TeNPs, and c) the supernatant of P. rubens, indicating the presence of different functional groups

Biological properties of colloidal nanosized selenium and tellurium particles

Antimicrobial properties

Well diffusion assay

Fig. 9 shows a schematic illustration of evaluation of antimicrobial properties of NPs using well diffusion assay. The antimicrobial efficacy of *P. rubens*-derived SeNPs and TeNPs against *E. coli*, *S. aureus*, and *C. albicans* were compared to the standard antibiotic gentamicin. As shown in

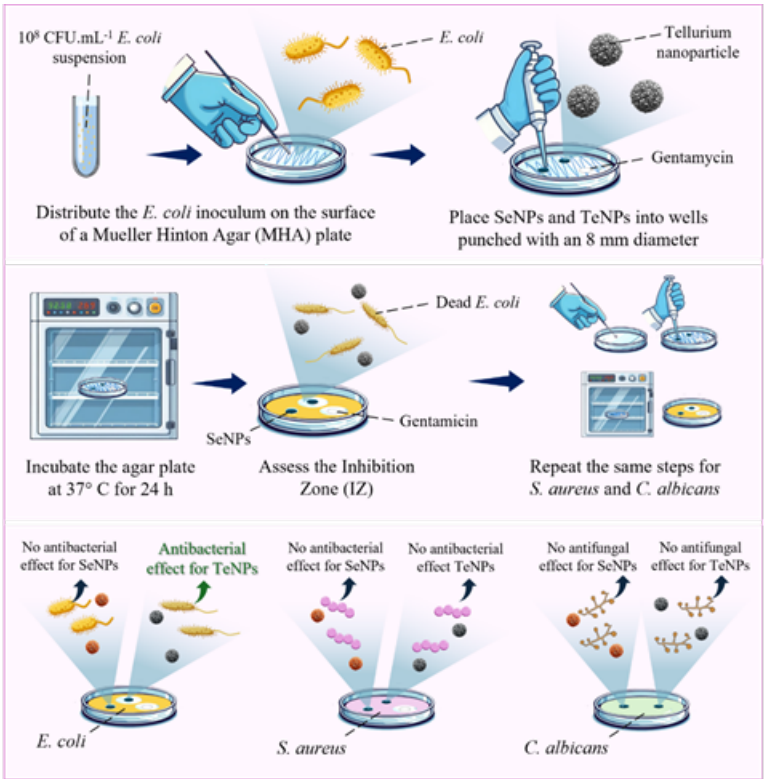

Fig. 9. A schematic illustration of evaluation of antimicrobial properties of nanosized selenium and tellurium particles using well diffusion assay representing the inhibition zone of TeNPs against *E. coli*

Table 1, the results revealed that the TeNPs were effective against gram-negative *E. coli* with an IZ of 27 mm. In contrast, no IZ was found for TeNPs against *S. aureus* at the tested concentration (100 µL of TeNPs per well from a stock solution of 1 mg.mL^{-1}). Surprisingly, no IZ was found for the SeNPs against *E. coli* and *S. aureus* at the tested concentration (100 µL of SeNPs per well from a stock solution of 1 mg.mL^{-1}). Moreover, the IZ was found to be around 21 mm for gentamicin against both *E. coli* and *S. aureus*. Furthermore, neither TeNPs nor SeNPs exhibited antifungal properties against *C. albicans* with the above-mentioned concentrations. Alternatively, in another investigation, it was stated that the *Aspergillus welwitschiae*-derived TeNPs with a Z-average of 114.8 nm exhibited no IZ against *C. albicans, Aspergillus niger*, and *Klebsiella* sp., when 100 µL of a stock of TeNPs with a concentration of 25 mg.mL^{-1} was transferred to a well of 1 cm diameter in cultured plates [33].

Broth microdilution assay

Fig. 10 shows a schematic illustration of evaluation of antimicrobial properties of NPs using broth microdilution assay. According to the results obtained from broth micro-dilution assay, TeNPs exhibited antibacterial properties against *E. coli*

Table 1. Antimicrobial assessment of SeNPs and TeNPs using well diffusion assay

Sample	Zone of inhibition (mm)		
	S. aureus	*E. coli*	*C. albicans*
TeNPs	0	27	0
SeNPs	0	0	0
Gentamicin (standard drug)	21	21	*NA

*NA: Not applicable

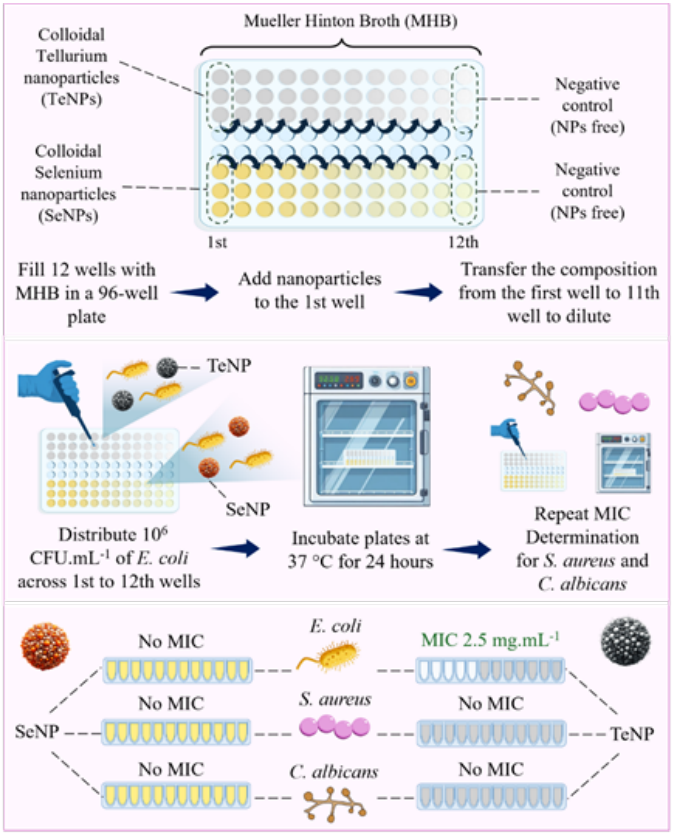

Fig. 10. A schematic illustration of evaluation of antibacterial properties of nanosized selenium and tellurium particles using broth microdilution assay representing the MIC of 2.5 mg.mL^{-1} of TeNPs against *E. coli*

with an MIC of 2.5 mg.mL^{-1}. However, gentamicin showed stronger antibacterial performance against *E. coli* with an MIC of 8 µg.mL^{-1}. There was no MIC found for SeNPs up to a concentration of 5 mg.mL^{-1} against *E. coli*. In addition, no MIC was found for SeNPs and TeNPs up to the concentration of 5 mg.mL^{-1} against *S. aureus* and *C. albicans*. Moreover, gentamicin had an MIC of 0.5 µg.mL^{-1} against *S. aureus*. In comparing our findings to previous studies, Vahidi et al. reported that *P. chrysogenum* (PTCC 5031)-derived TeNPs with a Z-average of 50.16 nm did not show antibacterial and antifungal properties based on broth micro-dilution assay up to a concentration of 250 µg.mL^{-1} of elemental Te against *S. aureus* (ATCC 25923), *E. coli* (ATCC 25922), *Staphylococcus epidermidis* (ATCC 12228), *Klebsiella pneumoniae* (ATCC 10031), *Saccharomyces cerevisiae* (PTCC 5269), and *C. albicans* (ATCC 10231) [20].

Quantitative evaluation of cell viability using flow cytometry

The sensitivity of *E. coli* to TeNPs was evaluated by measuring the percentages of live and dead *E. coli* cells. This was done after treating the cells with bioengineered TeNPs with the different concentrations, including MIC, 10*MIC, and 20*MIC. Additionally, the cells were treated with gentamicin with the concentrations of 10*MIC and 20*MIC. Flow cytometry was used for this measurement, and the results are shown in Fig. 11. The toxicity of TeNPs and gentamicin to *E. coli* cells was found to be dose-dependent. Fig. 11a depicts the untreated cells (negative control) with 99.2% live cells. Treatment with TeNPs at the concentrations of 2.5 (Fig. 11b), 25 (Fig. 11c), and 50 (Fig. 11d) mg.mL^{-1} resulted in 13.8%, 38.8%, and 52.1% cell death, respectively. Besides, treatment with gentamicin with the concentrations of 80 (Fig. 11e) and 160 µg.mL^{-1} (Fig. 11f) resulted in 30.2% and 46.5% cell death, respectively. The fundamental mechanism behind this was hypothesized to be the penetration of the fluorescent PI dye into injured microbial cells, where it interacts with DNA. This staining method allows for the detection of dead cells using a flow cytometer [34]. Fig. 12

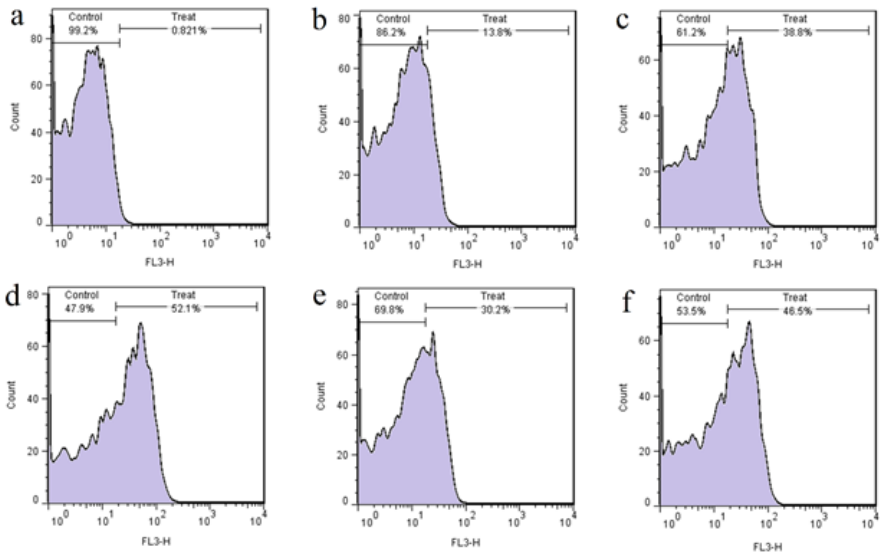

Fig. 11. The cell viability of *E. coli* was quantitatively evaluated using flow cytometry at concentrations of MIC, 10*MIC, and 20*MIC for biogenic TeNPs. The results are as follows: a) Untreated *E. coli* cells, serving as the negative control, exhibited 0.821% cell death; b) *E. coli* cells treated with TeNPs at the MIC concentration showed 13.8% cell death; c) *E. coli* cells treated with TeNPs at the 10*MIC concentration displayed 38.8% cell death; d) *E. coli* cells treated with TeNPs at the 20*MIC concentration exhibited 52.1% cell death; e) *E. coli* cells treated with gentamicin at the 10*MIC concentration showed 30.2% cell death; and f) *E. coli* cells treated with gentamicin at the 20*MIC concentration displayed 46.5% cell death

illustrates the possible antibacterial mechanisms of TeNPs. According to the literature, membrane damage is a key antibacterial mechanism of TeNPs. TeNPs are attracted to cell membranes, facilitating their penetration. Generation of ROS seems to be another antibacterial mechanism of TeNPs. In addition, TeNPs bind to DNA and potentially disrupt transcription. Moreover, the efficacy of the NPs in combating bacteria is significantly affected by their size, shape, and surface charge [35].

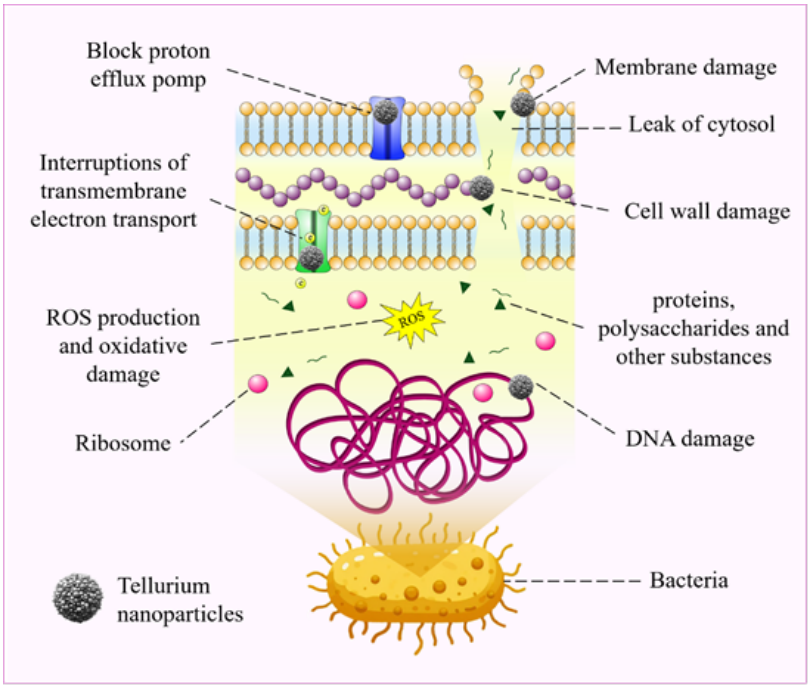

Fig. 12. A symbolic representation of the potential mechanisms underlying the antibacterial activity of TeNPs

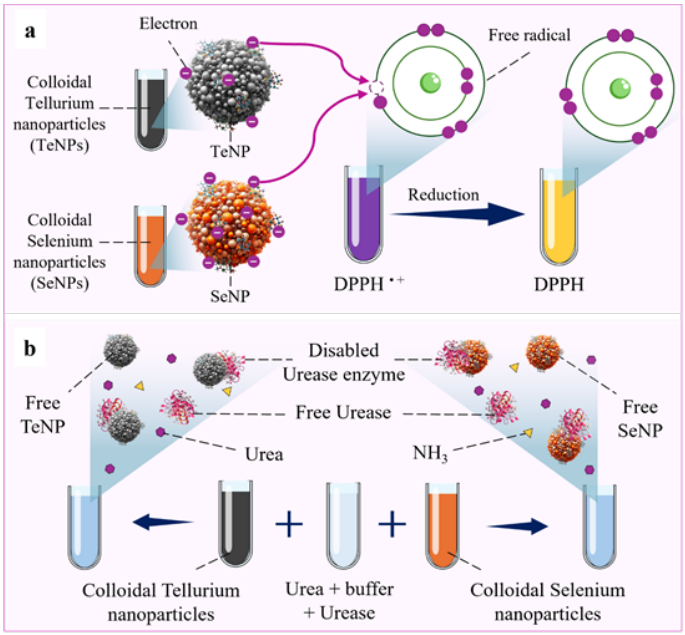

Fig. 13. a) A schematic illustration of antioxidant, and b) urease inhibitory activity of nanosized selenium and tellurium particles

Antioxidant properties

Fig. 13a shows a schematic illustration of antioxidant activity of SeNPs and TeNPs. The DPPH free radical scavenging experiment evaluated the antioxidant activity of TeNPs and SeNPs. Fig. 14a depicts the efficiency of the biogenic NPs at a concentration of 1 mg.mL^{-1} compared to the positive control vitamin C at a concentration of 10 mg.mL^{-1} and the supernatant of *P. rubens* (P<0.05). The mycosynthesized SeNPs had a stronger antioxidant effect than TeNPs by scavenging 57.93±2.20 and 43.90±1.98% of the DPPH free radicals, respectively. The biomolecules present in the fungal supernatant were suggested to play an essential role in the antioxidant activity of the mycosynthesized NPs since the supernatant itself exhibited 34.93±2.83% DPPH free radicals scavenging properties. Other scholars corroborated these results. For example, Vahidi et al. reported the mycofabrication of spherical-shaped TeNPs using *P. chrysogenum* (PTCC 5031). The biogenic NPs showed maximum inhibition of DPPH free radicals of 66.06±0.46% at a concentration of 500 µg.mL^{-1}, compared to 2500 µg.mL^{-1} of potassium tellurite (21.041±0.55%). The antioxidant effect was also found to be concentration-dependent [20]. Likewise, Nassar et al. used *Penicillium verhagenii* to fabricate of spherical-shaped SeNPs with a diameter of 25 to 75 nm. It was revealed the that green synthesized SeNPs could scavenge DPPH free radicals in a dose-dependent manner, showing maximum activity of 86.8±0.6% compared to the positive control, ascorbic acid, with 97.3±0.2% antioxidant potential, both at the concentrations of 1 mg.mL^{-1}. The authors suggested that the antioxidant effect of biogenic SeNPs could be due to the NPs transferring electrons to the free radical and enhancing the function of protective enzymes like glutathione peroxidase, thereby decreasing the harm attributed to free radicals toward cells [36]. In a similar study, SeNPs were mycosynthesized by *Penicillium expansum* and characterized as spherical with a mean diameter of 12.7 nm. The antioxidant property of biological SeNPs against DPPH free radicals was confirmed with an inhibition percentage of more than 50% at concentrations of more than 30 µg.mL^{-1} [37]. These findings suggested that the antioxidant properties of eco-friendly SeNPs and TeNPs have promising implications considered for human health maintenance after further clinical experiments.

Urease enzyme inhibitory properties

Fig. 13b shows a schematic illustration of urease inhibitory activity of SeNPs and TeNPs. Urease is an essential enzyme for the infectious ability of bacteria [38] and yeasts [39]. The present study examined the potential of *P. rubens*-mediated TeNPs and SeNPs at the concentrations of 0.5 and 1 mg.mL^{-1} to inhibit the function of the urease enzyme and control bacterial or fungal infections. Fig. 14b shows that biogenic TeNPs

were more effective against urease compared to SeNPs (P<0.05). Both TeNPs and SeNPs exhibited significant dose-dependent urease inhibitory activity (P<0.05). Thiourea was used as a positive control at a concentration of 10 mM, resulting in 95.85±1.60% urease inhibitory activity. In addition, the hindrance of urease activity by *P. rubens* supernatant was assessed to distinguish the urease inhibitory activity of the fungal-derived NPs and the fugal biofactory. The *P. rubens* supernatant exhibited only 10.58±2.42% urease inhibitory activity which was significantly less than the urease inhibitory activity of TeNPs and SeNPs (P<0.05). As far as we know, the urease inhibitory activity of biosynthesized SeNPs or TeNPs has not been investigated in other literature. However, various other biogenic metallic NPs have been found to inhibit urease effectively. For instance, Ahmad et al. confirmed the ability of *Piper cubeba*-mediated silver nanoparticles (AgNPs) to diminish the function of urease. The NPs, characterized as spherical with a diameter range between 40 and 80 nm, demonstrated the best inhibitory effect (78.6%) at a concentration of 0.05 mg. Furthermore, 5 mg of the plant extract and 0.5 mM of thiourea possessed the maximum inhibition of 88.5% and 95.2%, respectively [40]. In a separate study, phytofabricated nanosized gold particles (size distribution: 10 to 100 nm) represented urease inhibitory potential with an IC_{50} of 44.98±1.02 µg.mL^{-1} [41]. Similarly, Farooq et al. reported the plant-mediated fabrication of zinc nanoparticles (ZnNPs) using *Calotropis gigantea* with an irregular structure and a mean diameter ranging from 80 to 100 nm. The urease inhibitory assay revealed the significant potential of ZnNPs with an IC_{50} of 22.1 µM compared to that of thiourea (21.25 µM) [42]. Our findings suggest the potential role of green synthesized TeNPs and SeNPs as urease inhibitors *in-vitro* for further usage in medicine to assist preventive and therapeutic healthcare systems.

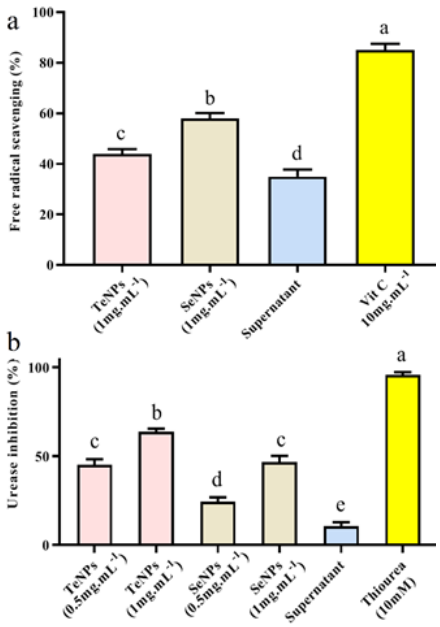

Fig. 14. a) DPPH free radical scavenging capacity of biologically fabricated TeNPs (43.90±1.98%) and SeNPs (57.93±2.20%) at a concentration of 1 mg.mL^{-1} compared to vitamin C (85.03%±2.47%) at the concentration of 10 mg.mL^{-1} and the fungal supernatant (34.93±2.83%); b) Urease inhibitory property of biosynthesized TeNPs and SeNPs at the concentration of 0.5 with inhibition percentages of 14±3.29% and 24.49±2.45%, respectively, and 1 mg.mL^{-1} with inhibition percentages of 63.81±1.69% and 46.95±3.39%, respectively, compared to thiourea (95.85±1.60%) at a concentration of 10 mM and fungal supernatant (10.58±2.42%). Data was reported as (Mean ± SD). A statistically significant difference between the groups that do not have a common letter was considered at a 95 confidence level (P<0.05)

Thrombolytic properties

As shown in Fig. 15a, SeNPs and TeNPs exhibited no significant thrombolytic performance

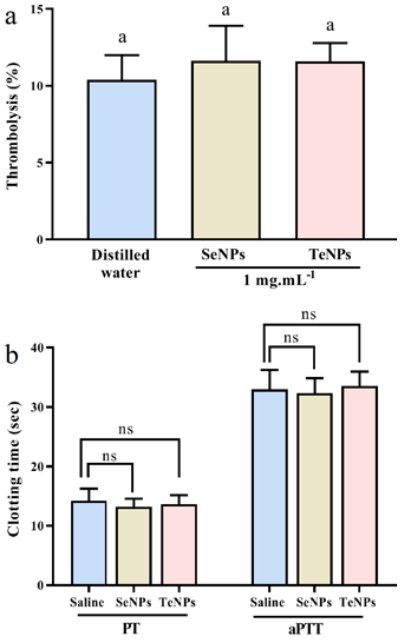

Fig. 15. a) Thrombolytic activity of SeNPs and TeNPs at a concentration of 1 mg.mL^{-1} compared to distilled water as negative control. Neither SeNPs nor TeNPs exhibited thrombolytic performance; b) The coagulation screening tests (aPTT and PT values) of SeNPs and TeNPs at a concentration of 1 mg.mL^{-1} compared to saline. Data was reported as (Mean ± SD). A statistically significant difference between the groups that do not have a common letter was considered at a 95 confidence level (P<0.05); ns refers to not significant (P>0.05); aPTT: activated partial thromboplastin time; PT: prothrombin time; SeNPs: selenium nanoparticles; TeNPs: tellurium nanoparticles

at a concentration of 1 mg.mL^{-1} compared to distilled water as a negative control (P>0.05). As far as we know, this is the first study to evaluate the thrombolytic potential of biosynthesized SeNPs and TeNPs.

Anticoagulant properties

As shown in Fig. 15b, SeNPs and TeNPs did not exhibit significant anticoagulant performance at a concentration of 1 mg.mL^{-1} compared to saline as a negative control (P>0.05). The average aPTT values for SeNPs, TeNPs, and saline (negative control) were 13.2±1.33, 13.65±1.47 and 14.19±2.01 s, respectively. In addition, the average PT values for SeNPs, TeNPs, and saline (negative control) were 32.34±2.56, 33.58±2.41 and 32.99±3.5 s, respectively. As far as we know, this study is the first to evaluate the anticoagulant potential of biosynthesized SeNPs and TeNPs.

CONCLUSION

The study presented in this report effectively demonstrates the extracellular mycofabrication of TeNPs and SeNPs with spherical morphology using the supernatant of *P. rubens*. The green fabricated nanosized selenium and tellurium particles ascertained considerable antioxidant and urease inhibitory performance. Moreover, the TeNPs exhibited significant antibacterial performance against *E. coli*. As far as we know, this study was the first to evaluate the anticoagulant, thrombolytic, and urease inhibitory activity of biosynthesized TeNPs and SeNPs. While the superior properties of biogenic TeNPs and SeNPs make them promising candidates for therapeutic agents in various fields, further examination is needed to fully understand their mechanisms of action and harness their full potential in addressing biomedical and environmental challenges. Therefore, their safety and efficacy should be clinically confirmed.

FUNDING

This work was supported by a grant from Shahid Beheshti University of Medical Sciences, Tehran, Iran (Grant Number 43008271).

DATA AVAILABILITY

No data was used for the research described in the article.

ETHICAL APPROVAL

Not applicable.

CONFLICT OF INTEREST

The authors declare no competing interests.

REFERENCES

1. Qamar SA, Asgher M, Khalid N, Sadaf M. Nanobiotechnology in health sciences: Current applications and future perspectives. Biocatal Agric Biotechnol. 2019; 22: 101388.
2. Pokrajac L, Abbas A, Chrzanowski W, Dias GM, Eggleton BJ, Maguire S, Maine E, Malloy T, Nathwani J, Nazar L. Nanotechnology for a sustainable future: Addressing global challenges with the international network for sustainable nanotechnology. ACS Publications; 2021; 15(12): 18608-18623.
3. Saleh TA. Nanomaterials: Classification, properties, and environmental toxicities. Environ Technol Innov. 2020; 20: 101067.
4. Salem SS, Fouda A. Green synthesis of metallic nanoparticles and their prospective biotechnological applications: An overview. Biol Trace Elem Res. 2021; 199: 344-370.
5. Gebreslassie YT, Gebretnsae HG. Green and cost-effective synthesis of tin oxide nanoparticles: A review on the synthesis methodologies, mechanism of formation, and their potential applications. Nanoscale Res Lett. 2021; 16(1): 97.
6. Harish V, Ansari MM, Tewari D, Yadav AB, Sharma N, Bawarig S, García-Betancourt M-L, Karatutlu A, Bechelany M, Barhoum A. Cutting-edge advances in tailoring size, shape, and functionality of nanoparticles and nanostructures: A review. J Taiwan Inst Chem Eng. 2023; 149: 105010.
7. Lee KX, Shameli K, Yew YP, Teow S-Y, Jahangirian H, Rafiee-Moghaddam R, Webster TJ. Recent developments in the facile bio-synthesis of gold nanoparticles (AuNPs) and their biomedical applications. Int J Nanomedicine. 2020; 275-300.
8. El-Seedi HR, El-Shabasy RM, Khalifa SA, Saeed A, Shah A, Shah R, Iftikhar FJ, Abdel-Daim MM, Omri A, Hajrahand NH. Metal nanoparticles fabricated by green chemistry using natural extracts: Biosynthesis, mechanisms, and applications. RSC Adv. 2019; 9(42): 24539-24559.
9. Madanayake NH, Adassooriya NM. Fungi-based synthesis of nanoparticles and its large-scale production possibilities. Mycosynth Nanomater: Perspect Challenges. 2023; 215.
10. Šebesta M, Vojtková H, Cyprichová V, Ingle AP, Urík M, Kolenčík M. Mycosynthesis of metal-containing nanoparticles—fungal metal resistance and mechanisms of synthesis. Int J Mol Sci. 2022; 23(22): 14084.
11. Iacovelli R, Bovenberg RA, Driessen AJ. Nonribosomal peptide synthetases and their biotechnological potential in Penicillium rubens. J Ind Microbiol Biotechnol. 2021; 48(7-8): kuab045.
12. Boruta T, Ścigaczewska A, Ruda A, Bizukojć M. Effects of the coculture initiation method on the production of secondary metabolites in bioreactor cocultures of Penicillium rubens and Streptomyces rimosus. Molecules. 2023; 28(16): 6044.
13. Conrado R, Gomes TC, Roque GS, De Souza AO. Overview of bioactive fungal secondary metabolites: Cytotoxic and antimicrobial compounds. Antibiotics. 2022; 11(11): 1604.
14. Venkatachalam P, Nadumane VK. Modulation of Bax and Bcl-2 genes by secondary metabolites produced by Penicillium rubens JGIPR9 causes the apoptosis of cancer cell lines. Mycology. 2021; 12(2): 69-81.
15. Li S-Y, Yang X-Q, Chen J-X, Wu Y-M, Yang Y-B, Ding Z-T. The induced cryptic metabolites and antifungal activities from culture of Penicillium chrysogenum by supplementing with host Ziziphus jujuba extract. Phytochemistry. 2022; 203: 113391.
16. Kisová Z, Šoltýsová A, Bučková M, Beke G, Puškárová A, Pangallo D. Studying the gene expression of Penicillium

rubens under the effect of eight essential oils. Antibiotics. 2020; 9(6): 343.
17. Din G, Hassan A, Dunlap J, Ripp S, Shah A. Cadmium tolerance and bioremediation potential of filamentous fungus Penicillium chrysogenum FMS2 isolated from soil. Int J Environ Sci Technol. 2021; 1-10.
18. Beleneva I, Kharchenko U, Kukhlevsky A, Boroda A, Izotov N, Gnedenkov A, Egorkin V. Biogenic synthesis of selenium and tellurium nanoparticles by marine bacteria and their biological activity. World J Microbiol Biotechnol. 2022; 38(11): 188.
19. Escobar-Ramírez MC, Castañeda-Ovando A, Pérez-Escalante E, Rodríguez-Serrano GM, Ramírez-Moreno E, Quintero-Lira A, Contreras-López E, Añorve-Morga J, Jaimez-Ordaz J, González-Olivares LG. Antimicrobial activity of Se-nanoparticles from bacterial biotransformation. Fermentation. 2021; 7(3): 130.
20. Vahidi H, Kobarfard F, Alizadeh A, Saravanan M, Barabadi H. Green nanotechnology-based tellurium nanoparticles: Exploration of their antioxidant, antibacterial, antifungal and cytotoxic potentials against cancerous and normal cells compared to potassium tellurite. Inorg Chem Commun. 2021; 124: 108385.
21. Zambonino MC, Quizhpe EM, Jaramillo FE, Rahman A, Santiago Vispo N, Jeffryes C, Dahoumane SA. Green synthesis of selenium and tellurium nanoparticles: Current trends, biological properties, and biomedical applications. Int J Mol Sci. 2021; 22(3): 989.
22. Imran M, Waqar S, Ogata K, Ahmed M, Noreen Z, Javed S, Bibi N, Bokhari H, Amjad A, Muddassar M. Identification of novel bacterial urease inhibitors through molecular shape and structure based virtual screening approaches. RSC Adv. 2020; 10(27): 16061-16070.
23. Devi CS, Mohanasrinivasan V, Tarafder A, Shishodiya E, Vaishnavi B, JemimahNaine S. Combination of clot buster enzymes and herbal extracts: A new alternative for thrombolytic drugs. Biocatal Agric Biotechnol. 2016; 8: 152-157.
24. Barabadi H, Mobaraki K, Jounaki K, Sadeghian-Abadi S, Vahidi H, Jahani R, Noqani H, Hosseini O, Ashouri F, Amidi S. Exploring the biological application of Penicillium fimorum-derived silver nanoparticles: *In vitro* physicochemical, antifungal, biofilm inhibitory, antioxidant, anticoagulant, and thrombolytic performance. Heliyon. 2023; 9(6): e16853.
25. Barabadi H, Kobarfard F, Vahidi H. Biosynthesis and characterization of biogenic tellurium nanoparticles by using Penicillium chrysogenum PTCC 5031: A novel approach in gold biotechnology. Iranian J Pharm Res: IJPR. 2018; 17(Suppl 2): 87.
26. Fardsadegh B, Jafarizadeh-Malmiri H. Aloe vera leaf extract mediated green synthesis of selenium nanoparticles and assessment of their *in vitro* antimicrobial activity against spoilage fungi and pathogenic bacteria strains. Green Process Synth. 2019; 8(1): 399-407.
27. Pyrzynska K, Sentkowska A. Biosynthesis of selenium nanoparticles using plant extracts. J Nanostruct Chem. 2022; 12(4): 467-480.
28. Zhang H, Zhou H, Bai J, Li Y, Yang J, Ma Q, Qu Y. Biosynthesis of selenium nanoparticles mediated by fungus Mariannaea sp. HJ and their characterization. Colloids Surf A Physicochem Eng Asp. 2019; 571: 9-16.
29. Feng X, Huang G, Qiu J, Peng L, Luo K, Liu D, Han P. Dynamic light scattering in flowing dispersion. Opt Commun. 2023; 531: 129225.
30. Mudalige T, Qu H, Van Haute D, Ansar SM, Paredes A, Ingle T. Chapter 11 - Characterization of nanomaterials: Tools and challenges. In: López Rubio A, Fabra Rovira MJ, Martínez Sanz M, Gómez-Mascaraque LG, editors. Nanomaterials for food applications. Elsevier; 2019. p. 313-353.
31. Danaei M, Dehghankhold M, Ataei S, Hasanzadeh Davarani F, Javanmard R, Dokhani A, Khorasani S, Mozafari MR. Impact of particle size and polydispersity index on the clinical applications of lipidic nanocarrier systems. Pharmaceutics. 2018; 10(2): 61.
32. Samimi S, Maghsoudnia N, Eftekhari RB, Dorkoosh F. Chapter 3 - Lipid-based nanoparticles for drug delivery systems. In: Mohapatra SS, Ranjan S, Dasgupta N, Mishra RK, Thomas S, editors. Characterization and biology of nanomaterials for drug delivery. Elsevier; 2019. p. 47-76.
33. Abo Elsoud MM, Al-Hagar OEA, Abdelkhalek ES, Sidkey NM. Synthesis and investigations on tellurium myconanoparticles. Biotechnol Rep. 2018; 18: e00247.
34. Trinh KTL, Lee NY. Recent methods for the viability assessment of bacterial pathogens: Advances, challenges, and future perspectives. Pathogens. 2022; 11(9): 1163.
35. Tang A, Ren Q, Wu Y, Wu C, Cheng Y. Investigation into the antibacterial mechanism of biogenic tellurium nanoparticles and precursor tellurite. Int J Mol Sci. 2022; 23(19): 11697.
36. Nassar ARA, Eid AM, Atta HM, El Naghy WS, Fouda A. Exploring the antimicrobial, antioxidant, anticancer, biocompatibility, and larvicidal activities of selenium nanoparticles fabricated by endophytic fungal strain Penicillium verhagenii. Sci Rep. 2023; 13(1): 9054.
37. Hashem AH, Khalil AMA, Reyad AM, Salem SS. Biomedical applications of mycosynthesized selenium nanoparticles using Penicillium expansum ATTC 36200. Biol Trace Elem Res. 2021; 199(10): 3998-4008.
38. Lin WF, Hu RY, Chang HY, Lin FY, Kuo CH, Su LH, Peng HL. The role of urease in the acid stress response and fimbriae expression in Klebsiella pneumoniae CG43. J Microbiol Immunol Infect. 2022; 55(4): 620-633.
39. Toplis B, Bosch C, Schwartz IS, Kenyon C, Boekhout T, Perfect JR, Botha A. The virulence factor urease and its unexplored role in the metabolism of Cryptococcus neoformans. FEMS Yeast Res. 2020; 20(4): foaa031.
40. Ahmad K, Asif HM, Afzal T, Khan MA, Younus M, Khurshid U, Safdar M, Saifulah S, Ahmad B, Sufyan A, Ansari SA, Alkahtani HM, Ansari IA. Green synthesis and characterization of silver nanoparticles through the Piper cubeba ethanolic extract and their enzyme inhibitory activities. Front Chem. 2023; 11: 1065986.
41. Alhumaydhi FA. Green synthesis of gold nanoparticles using extract of Pistacia chinensis and their *in vitro* and *in vivo* biological activities. J Nanomater. 2022; 2022: 5544475.
42. Farooq A, Khan UA, Ali H, Sathish M, Naqvi SA, Iqbal H, Ali H, Mubeen I, Amir MB, Mosa WFA, Baazeem A, Moustafa M, Alrumman S, Shati A, Negm S. Green chemistry based synthesis of zinc oxide nanoparticles using plant derivatives of Calotropis gigantea (giant milkweed) and its biological applications against various bacterial and fungal pathogens. Microorganisms. 2022; 10(11): 2195.